Antibiotic treatment enhances the genome-wide mutation rate of target cells

Hongan Long[a], Samuel F. Miller[a], Chloe Strauss[a], Chaoxian Zhao[b], Lei Cheng[c], Zhiqiang Ye[a], Katherine Griffin[a], Ronald Te[a], Heewook Lee[d], Chi-Chun Chen[a], and Michael Lynch[a,1]

[a]Department of Biology, Indiana University, Bloomington, IN 47405; [b]Department of Biology, School of Life Sciences, East China Normal University, Shanghai, China 200241; [c]Heilongjiang River Fisheries Research Institute, Chinese Academy of Fishery Sciences, Harbin, Heilongjiang Province, China 150001; and [d]School of Informatics and Computing, Indiana University, Bloomington, IN 47405

Contributed by Michael Lynch, March 23, 2016 (sent for review January 22, 2016; reviewed by Roderick Craig MacLean and Ivan Matic)

Although it is well known that microbial populations can respond adaptively to challenges from antibiotics, empirical difficulties in distinguishing the roles of de novo mutation and natural selection have left several issues unresolved. Here, we explore the mutational properties of *Escherichia coli* exposed to long-term sublethal levels of the antibiotic norfloxacin, using a mutation accumulation design combined with whole-genome sequencing of replicate lines. The genome-wide mutation rate significantly increases with norfloxacin concentration. This response is associated with enhanced expression of error-prone DNA polymerases and may also involve indirect effects of norfloxacin on DNA mismatch and oxidative-damage repair. Moreover, we find that acquisition of antibiotic resistance can be enhanced solely by accelerated mutagenesis, i.e., without direct involvement of selection. Our results suggest that antibiotics may generally enhance the mutation rates of target cells, thereby accelerating the rate of adaptation not only to the antibiotic itself but to additional challenges faced by invasive pathogens.

antibiotic resistance | mutation rate | resistance evolution | DNA repair | low-fidelity polymerases

The emergence of antibiotic resistance in pathogenic bacteria poses a major threat to human health, with de novo mutations being one important source for heritable resistance acquisition (1). As a consequence of the widespread use of antibiotics in human disease prevention and promotion of livestock growth, sublethal antibiotic concentrations are now common in the environment, and there is substantial evidence that resistant bacterial strains are successfully moving across host species boundaries (2–5). Although such observations raise significant public-policy concerns (6), our knowledge of the mutational processes underlying bacterial acquisition of resistance under low levels of antibiotic exposure is quite limited. Particularly lacking is information on the influence of antibiotics on the mutation rate itself, as opposed to the downstream ability of natural selection to promote resistance mutations.

Bacteria deficient in postreplicative DNA mismatch repair (MMR) are of special interest in the context of antibiotic-resistance acquisition, as such strains typically have mutation rates elevated by ∼100 times (7, 8). For example, ∼36% of cystic fibrosis patients chronically infected by the pathogen *Pseudomonas aeruginosa* are colonized by mutator strains, many of which are antibiotic resistant (9). Although mutator strains can have long-term disadvantages, owing to the accumulation of harmful mutations (10), in the face of strong selective challenges, the short-term benefits of resistance mutations can take precedence, leading to antibiotic treatment failure for infectious diseases (11). However, there have been only a few empirical comparisons of resistance evolution in mutator vs. nonmutator lines under long-term sublethal antibiotic exposure (12, 13).

Among antibiotics that promote the evolution of resistance, fluoroquinolones such as norfloxacin are of particular concern because they directly interfere with DNA replication by binding gyrase or topoisomerase IV (14–16), and hence may encourage replication errors that are the major source of mutations (17). Gyrases bound with fluoroquinolone molecules result in cross-linked protein–DNA complexes containing broken DNA that induces the SOS response (18–20). Three error-prone DNA polymerases are expressed in *Escherichia coli* during the SOS response, substantially elevating the mutation rate (21, 22). Under sustained exposure to norfloxacin, mutation rates revealed by reporter constructs can be elevated 2–9 times (18, 23). Norfloxacin is also thought to elevate intracellular reactive oxygen species (ROS) levels (24, 25), which may further increase the rate of genomic mutation and the subsequent rate of acquisition of multidrug resistance (23, 26).

To date, all studies of the effects of broad-spectrum antibiotics on genome stability have relied on the use of reporter constructs. Such approaches are attractive because they allow the detection of mutations without sequencing (through observations of growth in otherwise nonpermissible conditions). However, although follow-up targeted sequencing can reveal the molecular nature of the induced mutations, reporter constructs are problematical because (*i*) not all mutations are always traceable to the target locus; (*ii*) the subset of detectable mutations is restricted to a narrow genomic context (sometimes only a few nucleotide sites), rendering the results susceptible to context dependence issues (27, 28); and (*iii*) numerous analytical assumptions need to be made to account for the large subset of undetectable mutations (29, 30).

Significance

The evolution of antibiotic resistance by pathogenic bacteria poses a major challenge for human health. Whereas it is clear that natural selection promotes resistance-conferring mutations, our understanding of the response of the mutation rate to antibiotics is limited. With hundreds of *Escherichia coli* cell lines evolving in a near-neutral scenario under exposure to the fluoroquinolone norfloxacin, this study reveals a significant linear relationship between the mutation rate and antibiotic concentration, while also demonstrating that antibiotic treatment compromises the efficiency of DNA oxidative-damage repair and postreplicative mismatch repair. Thus, antibiotics not only impose a selective challenge to target and off-target bacteria but also accelerate the rate of adaptation by magnifying the rate at which advantageous mutations arise.

Author contributions: H. Long designed research; H. Long, S.F.M., C.S., C.Z., L.C., K.G., and R.T. performed research; H. Long, Z.Y., H. Lee, C.-C.C., and M.L. analyzed data; and H. Long and M.L. wrote the paper.

Reviewers: R.C.M., University of Oxford; and I.M., INSERM U1001, Génétique Moléculaire Evolutive et Médicale.

The authors declare no conflict of interest.

Data deposition: The sequence reported in this paper has been deposited in the National Center for Biotechnology Information Sequence Read Archive (BioProject no. PRJNA301160; study no. SRP066119).

[1]To whom correspondence should be addressed. Email: milynch@indiana.edu.

This article contains supporting information online at www.pnas.org/lookup/suppl/doi:10.1073/pnas.1601208113/-/DCSupplemental.

These types of limitations can be avoided entirely by whole-genome sequencing (WGS) of lines generated in mutation accumulation (MA) experiments. MA experiments using bacteria are performed by repeatedly passing large numbers of initially identical lines through single-cell bottlenecks, a procedure that prevents natural selection from promoting or eradicating nearly all mutations, except the small subset with extremely large effects (31). This MA/WGS procedure provides an essentially unbiased, genome-wide view of the rate and full molecular spectrum of mutations, and has yielded accurate estimates of these features in a wide variety of prokaryotic and eukaryotic microbes (27, 28, 32–34).

Here, we apply the MA/WGS strategy to characterize the rate and molecular spectrum of genomic mutations produced by three sets of *E. coli* MA lines exposed to a wide range of sublethal norfloxacin concentrations. In addition to performing assays on wild-type K-12 MG1655, which has a representative background mutation rate for a prokaryote (27, 35), we performed parallel assays with a MMR-deficient mutator strain (Δ*mutS*), as well as with an adenine DNA glycosylase-deficient strain (Δ*mutY*) to evaluate the potential role of oxidative damage of nucleotides. Our results provide quantitative insight into the relationship between antibiotic concentration and the rate and molecular spectra of mutations in the target species, the degree to which DNA oxidation is involved, and the extent to which elevated mutation rates accelerate the rate of resistance acquisition.

Results

We explored how *E. coli* mutation rates change when treated with sublethal levels of norfloxacin after first predetermining the range of applicable sublethal concentrations of the drug. We exposed the three progenitor strains with 10 concentrations of norfloxacin, incubating ∼1,500 cells on LB plates at 37 °C for 24 h, then counting the colony-forming units to estimate the efficiency of plating (EOP) by dividing treatment colony-forming units by that without norfloxacin. The EOP, which reflects the proportion of cells not inhibited by norfloxacin, decreases with increasing norfloxacin concentration (Fig. 1). The EOP of the Δ*mutY* strain at intermediate norfloxacin concentrations is higher than either the wild-type or the Δ*mutS* (MMR$^-$) strain (paired *t* test, $P < 0.05$), indicating that loss of *mutY* is protective against antibiotics at sublethal or higher doses (36).

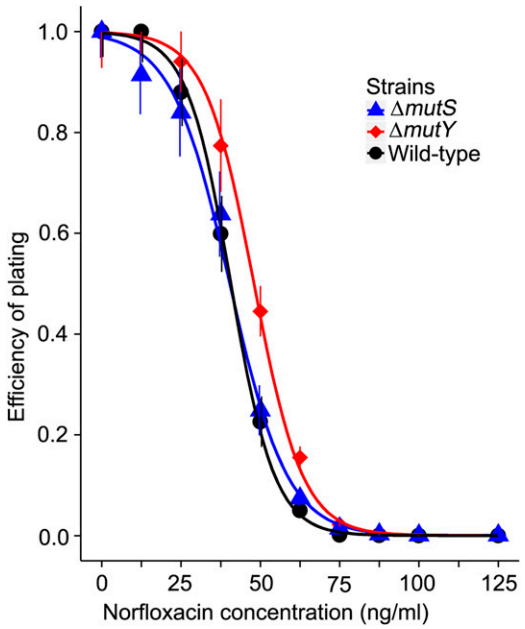

Fig. 1. Efficiency of plating (EOP) of strains under different norfloxacin concentrations. The plotted lines are logistic regressions. Bars denote SEM.

Mutation Rates Are Strongly Correlated with Norfloxacin Concentrations. From the wild-type progenitor cell, we created eight treatment groups of MA lines and grew 48 replicate lines per group on LB plates with a standard daily streak-and-plate procedure. The norfloxacin doses applied (0, 12.5, 25, 37.5, 50, 62.5, 75, and 87.5 ng/mL) are orders of magnitude lower than peak norfloxacin concentrations in the serum of patients after taking a clinical dosage (37). After ∼2 mo of daily single-colony transfers for each of the 384 lines, we sequenced whole genomes and ascertained the acquired mutations in each final evolved line (Table 1 and Dataset S1, Tables S1–S3). Mutation rates involving single base pair substitutions (BPSs) across the genome exhibit a strong linear increase with norfloxacin dose (Pearson's product-moment correlation coefficient $r = 0.94$, $P = 0.0006$), with the highest concentration yielding ∼4.0 times elevation relative to the control (Fig. 2*A*). The mutation rates to small-sized insertions/deletions (<19 bp) also increase with norfloxacin treatment in both the wild-type and Δ*mutS* lines (Fig. S1), although as is usually seen in bacterial mutation assays (27), such mutations are only on average 11% as abundant as BPS mutations.

Genetic drift in single-cell bottlenecked lines of *E. coli* is strong enough to prevent the operation of selection on all but mutations with very large effects (31), and numerous prior studies of this sort have validated the effectively nonselective nature of MA experiments (27, 28, 33, 38, 39). However, to directly test whether selection might have biased the mutation rate/spectrum (e.g., by enriching for mutations conferring norfloxacin resistance), we examined the synonymous and nonsynonymous status of each coding-region BPS (Dataset S1, Table S2). For no treatment is the nonsynonymous/synonymous BPS ratio significantly different from that of the nontreatment control (χ^2 test, $P > 0.05$ in all cases), indicating that the vast majority of acquired amino acid-altering BPSs were not selectively promoted by norfloxacin treatment but simply accumulated in a neutral fashion. As noted below, this conclusion is also confirmed by the very low incidence of enriched BPSs in resistance-associated genes.

Because nucleotide changes at fourfold degenerate sites do not cause an amino acid change, whereas most resistance mutations likely involve amino acid changes, as a final check for selection bias, we calculated BPS mutation rates exclusively at fourfold degenerate sites. These rates strongly correlate with norfloxacin concentration ($r = 0.97$, $P = 6.34 \times 10^{-5}$; Fig. 2*A*), yielding a pattern not significantly different from that for rates derived from all genomic sites (two-sample Kolmogorov–Smirnov test, $D = 0.25$, $P = 0.98$). Examination of the spectrum of norfloxacin-induced BPS mutations shows that the mutation rates of all possible BPS categories increase significantly with norfloxacin doses (Fig. 2*B* and Dataset S1, Table S4), which contrasts with the transversion-dominant spectra of previously reported SOS-dependent mutagenesis (40, 41), implying the operation of mutagenesis mechanisms beyond a simple SOS response during norfloxacin treatment. Thus, we conclude that genome-wide BPS mutation rates increase with sublethal concentrations of norfloxacin. Moreover, the linear relationship between the BPS mutation rate and dosage indicates an absence of saturation in the response for the range of concentrations applied, suggesting that higher doses will elicit still higher mutation rates.

Because the MMR pathway repairs multiple types of pre-mutations in wild-type lines (27, 42), the contrast between mutation spectra in MMR-deficient and wild-type strains can be used to reveal early-stage mutagenic effects (i.e., before MMR removal). Therefore, we performed a MA/WGS analysis of lines originating from a single MMR$^-$ cell (with the critical *mutS* gene deleted, which yields ∼104 times BPS mutation rate elevation over the wild-type level) (Dataset S1, Tables S1 and S5–S7). The

Table 1. Summary of MA line information

Strains	Concentration	*N*	Cell divisions	Ts	Tv	N_e	Insertions	Deletions	MIC (SEM)
+	0 (A)	46	1,682	42	37	14.0	1	8	121.38 (2.08)
+	12.5 (B)	48	1,687	54	41	14.0	10	8	125.00 (0)
+	25 (C)	48	1,612	60	58	13.5	5	15	125.43 (2.36)
+	37.5 (D, XD)	47	1,254	68	62	12.5	6	16	142.73 (5.91)
+	50 (E)	47	1,277	98	76	11.5	11	12	177.75 (15.26)
+	62.5 (F)	45	1,274	97	95	11.5	9	21	202.78 (15.08)
+	75 (G)	46	1,221	117	111	11.0	12	22	229.17 (26.57)
+	87.5 (H)	48	1,229	102	79	11.0	9	24	205.73 (12.62)
Δ*mutS*	0 (SA)	12	763	950	19	14.0	105	79	149.31 (27.72)
Δ*mutS*	12.5 (SB)	12	750	1,070	25	14.0	116	58	133.68 (17.48)
Δ*mutS*	25 (SC)	12	702	1,076	40	13.5	118	90	151.07 (16.45)
Δ*mutS*	37.5 (SD)	12	1,526	2,249	139	12.5	184	143	263.89 (47.38)
Δ*mutS*	50 (SE)	12	696	1,221	49	13.5	139	108	395.83 (73.16)
Δ*mutS*	62.5 (SF)	12	667	955	39	13.0	103	62	338.92 (60.93)
Δ*mutS*	75 (SG)	12	662	1,437	65	13.0	182	101	322.94 (51.59)
Δ*mutS*	87.5 (SH)	12	572	1,114	51	12.0	153	112	361.11 (36.02)
Δ*mutY*	0 (YA)	15	2,023	23	211	14.5	2	4	—
Δ*mutY*	3.125 (YB)	19	1,972	26	276	14.0	2	3	—
Δ*mutY*	12.5 (YC)	19	2,008	30	286	14.5	4	1	—
Δ*mutY*	50 (YF)	18	1,735	85	245	12.5	11	19	—
Δ*mutY*	H_2O_2 (+)	20	1,291	104	1,403	13.5	2	14	—
Δ*mutY*	25 (YD)	43	756	26	350	13.5	4	6	—
Δ*mutY*	37.5 (YE)	46	713	31	336	13.0	1	8	—
Δ*mutY*	75 (YG)	46	603	53	343	11.5	6	9	—
Δ*mutY*	87.5 (YH)	40	622	90	292	11.5	10	19	—

Norfloxacin concentration ("Concentration") and MIC are in units of nanograms per milliliter norfloxacin. Cell divisions, the average number of cell divisions per line; Insertion and Deletion, the total numbers of insertion/deletion (<19 bp) mutations detected across all lines in the group; MIC, minimum inhibitory concentration of the final evolved lines; *N*, number of lines in the group; N_e, effective population size; SEM, standard error of the mean; Ts, number of transitions in the group; Tv, number of transversions; +, wild type. The letters in parentheses in the Concentration column are group labels.

strong correlation between the BPS mutation rate and the norfloxacin concentration remains in the mutator lines, with ∼1.85 times increase over the full range of concentrations within the MMR$^-$ lines (Fig. 2*C* and Dataset S1, Table S4).

As seen in previous work on background mutational features in *E. coli* (27), there are substantial differences in the mutation spectra of wild-type and MMR$^-$ lines (Fig. 2 *B* and *D*). Most notably, the transition/transversion ratio of mutations is much higher in the latter, and also scales negatively with norfloxacin concentration, whereas there is no correlation detected in the wild-type lines (Fig. 3*A*). The pattern observed in MMR$^-$ lines is likely shaped by norfloxacin induction of the SOS response (see next section), which elevates the relative incidence of transversion mutations (43).

The ratio of mutation rates in MMR$^+$ and MMR$^-$ backgrounds, a measure of the fraction of premutations not eliminated by MMR, is positively correlated with norfloxacin concentration ($r = 0.86$, $P = 0.007$), increasing from 0.009 in the absence of norfloxacin to 0.019 at the highest dose. Although this is a small quantitative change, it suggests that the MMR pathway may become progressively overwhelmed as the baseline rate of production of premutations increases.

Mutation Rate vs. Expression of Low-Fidelity DNA Polymerases Under Norfloxacin Treatment. To explore whether the mutation rate increase induced by norfloxacin is an indirect physiological response to stress, e.g., SOS gene expression, we measured expression levels for the entire transcriptomes of both the wild-type and MMR$^-$ progenitor lines over the range of norfloxacin concentrations used in the MA studies. In both the wild-type and MMR$^-$ strains, expression of the hallmark gene *sulA* involved in SOS induction (44) is significantly elevated with norfloxacin concentration (Dataset S1, Tables S8–S11). A gene pathway enrichment analysis further shows that expression of the SOS response pathway is significantly elevated above the background level in each norfloxacin treatment of the wild-type and MMR$^-$ strains (Dataset S1, Table S12).

Excision of the lambdoid prophage element e14 is known to occur upon SOS response activation (45). Using both sequencing depth and paired-end read information, we detected widespread excision of e14 in the wild-type and MMR$^-$ MA lines exposed to norfloxacin (Dataset S1, Tables S1 and S5), with a significant correlation between e14 excision rates and norfloxacin concentrations in both sets of lines (Fig. 3*B*). None of the wild-type or MMR$^-$ control lines experienced e14 excision (Dataset S1, Tables S1 and S5). We also observed partial deletions of another prophage CP4-6 in norfloxacin-treated wild-type and MMR$^-$ lines (Fig. S2). These ∼11.5-kb deletions are flanked by IS1 insertion elements, which are known to cause deletions through recombination (46). By contrast, the transposition rate of insertion sequences did not change across treatment levels in either the wild-type or MMR$^-$ lines (Dataset S1, Table S13), which is consistent with a lack of elevated expression for the DNA-mediated transposition pathway in any norfloxacin treatment (Dataset S1, Table S12).

Expression levels of the low-fidelity DNA polymerases pol II, IV, and V are positively correlated with the mutation rate in the wild-type lines, but not in the MMR$^-$ lines (Fig. 3 *C* and *D*, and Dataset S1, Tables S8 and S10). The decreased correlation in the latter case suggests that a large proportion of mutations in the MMR$^-$ lines are products of mechanisms unassociated with low-fidelity polymerases and that MMR normally repairs. Such mechanisms may be associated with transition premutations

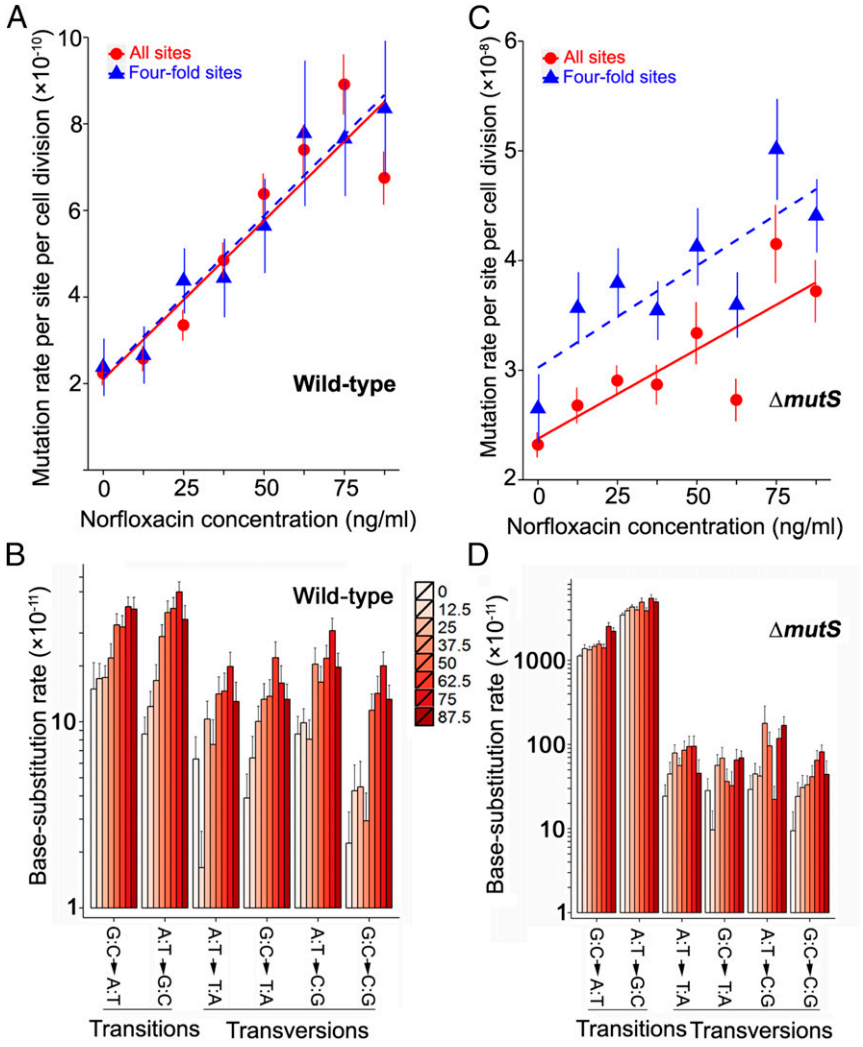

Fig. 2. Base substitution mutation rates. (*A*) Mutation rates of wild-type lines treated with different doses of norfloxacin. Regression of the mutation rate at fourfold degenerate sites (*Y*) vs. norfloxacin concentration (*X*): $Y = (7.46 \times 10^{-12})X + (2.15 \times 10^{-10})$; $r = 0.94$, $P = 0.0006$ for all sites, and $r = 0.97$, $P = 0.00006$ for fourfold degenerate sites. Vertical bars denote SEM. (*B*) Mutation spectra of wild-type lines treated with different doses, as indicated by the gradient scale. G:C→A:T denotes G→A and C→T mutations, with similar definitions for other *x*-axis labels. (*C*) MMR$^-$ line mutation rates. Regression function $Y = (1.86 \times 10^{-10})X + (3.02 \times 10^{-8})$ for fourfold degenerate sites; $r = 0.83$, $P = 0.01$ for all sites; $r = 0.84$, $P = 0.009$ for fourfold degenerate sites. (*D*) Mutation spectra of Δ*mutS* lines.

generated by the major polymerases Pol I and III (47) and the intrinsic transition repair bias of MMR (48).

Norfloxacin Affects DNA Oxidative Damage Repair. The reduced efficiency of MMR associated with increasing norfloxacin treatment inspires the idea that other DNA repair pathways may also be compromised by antibiotic treatment. Motivated by the observation that the wild-type G:C→T:A transversion rate is strongly elevated by norfloxacin treatment ($r = 0.77$, $P = 0.02$; Fig. 2*B*), we conducted MA experiments with a Δ*mutY* strain to determine whether antibiotic treatment affects DNA oxidative-damage repair. The Δ*mutY* strain is dysfunctional in recognizing adenines mispaired with 8-oxo-guanines (49), and it is known that the failure to recognize and remove 8-oxo-guanines residing in DNA elevates the postreplication G:C→T:A transversion mutation rate (50–52).

We performed two sets of MA experiments using lines originating from a single-cell Δ*mutY* progenitor, encompassing the full range of norfloxacin concentrations noted above as well as a treatment of 20 mM H_2O_2 (but no norfloxacin). The latter treatment was imposed to verify that high oxidative conditions do indeed elevate the mutation rate; if the resultant mutation rate is elevated relative to that under norfloxacin treatment (which it is), a lack of elevated G:C→T:A mutation rate must not be due to baseline saturation with oxidation damage. The highest norfloxacin concentration used in the first experiment was 50 ng/mL, and the second experiment started at 25 ng/mL and expanded the treatment range to the highest levels of norfloxacin concentrations used in earlier experiments.

G:C→T:A mutation rates in Δ*mutY* lines do not covary with norfloxacin concentrations (two-way ANOVA with experimental set and concentration as the two categories, $P_{\text{concentration}} = 0.25$; Dataset S1, Tables S14–S17). This suggests that, although there is a positive response of the rate of G:C→T:A transversion mutations to norfloxacin dosage in wild-type lines, this is not a consequence of the direct promotion of DNA oxidative damage by norfloxacin, but rather an indirect effect of the influence of norfloxacin on the repair systems that normally inhibit G:C→T:A mutations, i.e., DNA oxidative-damage repair. This hypothesis is supported by the observation that MutY is down-regulated by antibiotic-promoted oxidative stress in *E. coli* (23, 53), perhaps because this attenuates the deleterious effect of MutY activity on

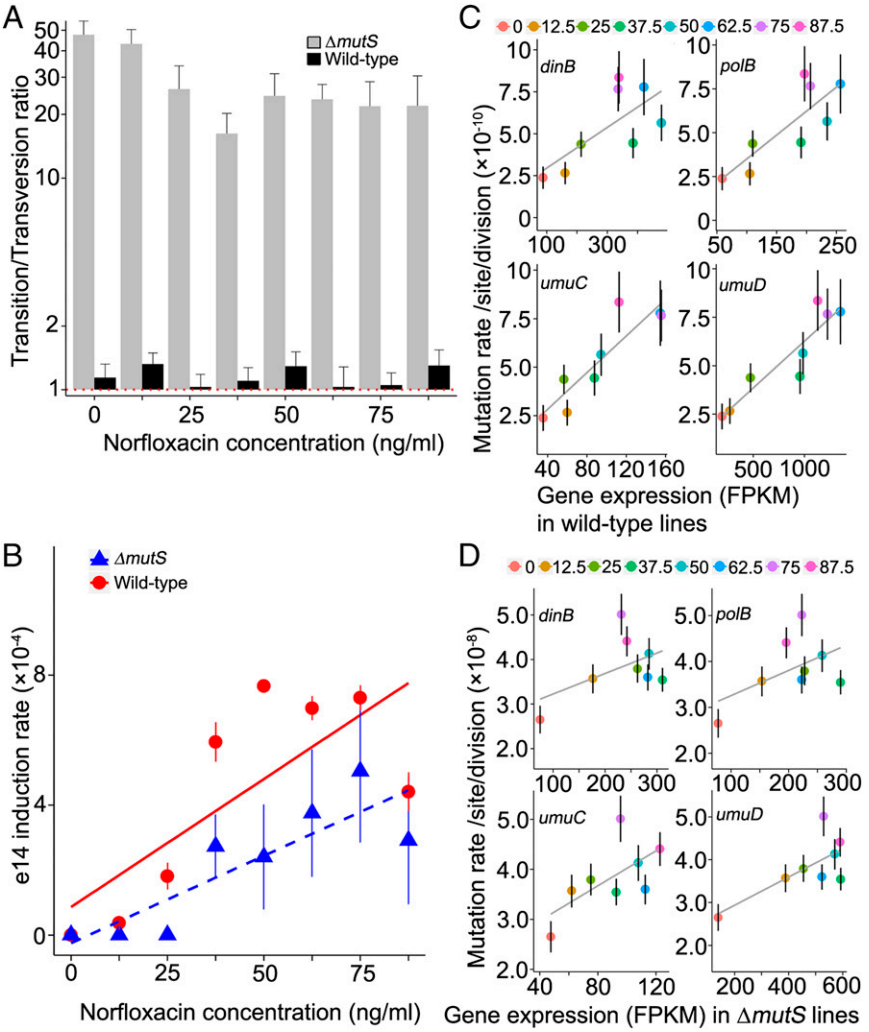

Fig. 3. Mutation and gene expression patterns across norfloxacin treatments. (*A*) Transition/transversion ratios of wild-type and Δ*mutS* (MMR⁻) lines at different concentrations; red dotted line shows ratio of 1; correlation test of ratio vs. concentrations: $r = -0.75$, $P = 0.03$ for Δ*mutS;* $r = -0.01$, $P = 0.98$ for wild type. (*B*) e14 induction rate per line per cell division in the wild-type and Δ*mutS* lines: $r = 0.76$, $P = 0.03$ for wild-type lines; $r = 0.86$, $P = 0.006$ for MMR⁻ lines. (*C*) Wild-type mutation rate at fourfold degenerate sites vs. expression levels of low-fidelity DNA polymerases in the SOS pathway; color legends show norfloxacin concentrations in units of nanograms per milliliter; gray lines are linear regressions: $r = 0.82$, $P = 0.01$ for *polB* (pol II); $r = 0.70$, $P = 0.05$ for *dinB* (pol IV); $r = 0.90$, $P = 0.002$ for *umuC* (pol V); $r = 0.92$, $P = 0.001$ for *umuD* (pol V). (*D*) The mutation rate at fourfold degenerate sites in Δ*mutS* lines vs. expression levels of low-fidelity polymerases: $r = 0.52$, $P = 0.19$ for *polB* (pol II); $r = 0.50$, $P = 0.21$ for *dinB* (pol IV); $r = 0.65$, $P = 0.08$ for *umuC* (pol V); $r = 0.72$, $P = 0.04$ for *umuD* (pol V). FPKM, fragments per kilobase of transcript per million mapped reads.

damaged DNA (36) (Fig. 1). Interestingly, the G:C→T:A transversion mutations in Δ*mutY* lines distribute in a nonrandom wave-like pattern across the genome (Fig. S3).

Very Few Genes Are Enriched with Mutations. Although we have shown that selection for norfloxacin resistance has a negligible influence on our mutation rate estimates, given the number of mutations harvested in this analysis (Table 1), there remains a possibility of enrichment of mutations in a small number of genes, including those that are relevant to antibiotic resistance. To determine whether any changes in sensitivity to norfloxacin occurred in the MA lines, we measured the minimum inhibitory concentration (MIC) for all wild-type and MMR⁻ lines (Dataset S1, Tables S1 and S5). Despite the extreme reduction in the efficiency of selection under the MA design, there is a trend toward increasing resistance with norfloxacin concentration to the point of an approximate doubling at the highest dosage (Table 1), and the MMR⁻ lines develop stronger resistance than wild-type lines at higher concentrations (Fig. 4). Notably, two MMR⁻ lines (SA6 and SA12; Dataset S1, Table S5) grown in the absence of norfloxacin exhibited a ≥2 times increase in MIC, showing that resistance can sometimes be enhanced solely by an accelerated mutation rate without any direct involvement of selection. In both the wild-type and MMR⁻ MA lines, we also observe some MICs lower than that of the progenitor MIC, all in <37.5 ng/mL treatments (Dataset S1, Tables S1 and S5), showing that mutations have arisen that both increase and decrease norfloxacin resistance.

To determine whether specific genes were enriched with mutations conferring resistance, we pooled the BPS mutations in the coding regions for all genes in the wild-type lines treated with norfloxacin (787 BPSs in 674 genes), as well as those within the treated MMR⁻ lines (8,229 BPSs in 3,144 genes). Then, for each gene, we calculated the Poisson probability of seeing greater than or equal to the number of observed mutations in the gene given the expected mutation rate of the gene with norfloxacin treatment. The expected mutation rate of the gene was calculated as the product of the average per base mutation rate in

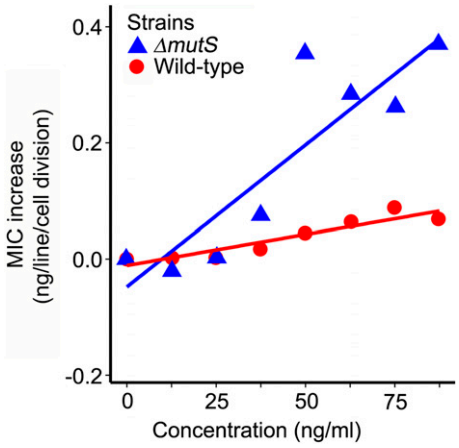

Fig. 4. Average norfloxacin resistance increase of wild-type and Δ*mutS* mutator lines treated with different concentrations. The average resistance increase is calculated as follows: (mean MIC of the treated lines – mean MIC of the 0 ng/mL control)/(average number of cell divisions per line in the treatment). Correlation: $r = 0.93$, $P = 0.0009$ for wild type; $r = 0.89$, $P = 0.003$ for Δ*mutS*.

norfloxacin-treated lines (4.54×10^{-10} for wild type; 3.19×10^{-8} for MMR$^-$) and the gene length (Dataset S1, Tables S18 and S19). After Bonferroni correction for multiple comparisons (corrected P values: wild type, 7.42×10^{-5}; MMR$^-$, 1.59×10^{-5}), significant mutation rate elevation is suggested in three [multiple antibiotic resistance operon repressor (*marR*); DNA gyrase subunit B (*gyrB*); DNA gyrase subunit A (*gyrA*)] and two genes [positive regulator of the AcrAB multidrug resistance efflux pump (*sdiA*); *gyrA*] in the wild-type and MMR$^-$ lines, respectively (Dataset S1, Tables S18 and S19; *mdaB* was removed from the wild-type gene list because its mutations reside only in lines with nonelevated MICs). In sum, only 2.2% of wild-type and 0.4% of MMR$^-$ BPSs are in genes that possibly experienced selection for resistance.

Only *gyrA* appears on the candidate lists for both the wild-type and MMR$^-$ lines, suggesting that either these two types of lines experience different paths to resistance, or that there are some false positives in this analysis. Most mutated gyrase genes contain only a single mutation (Dataset S1, Table S20), but lines containing at least one gyrase mutation have an average MIC increase of 2.5 times, suggesting that such mutations do specifically confer resistance, although two or more mutations are usually required for resistance to high doses (54). Another known norfloxacin target, topoisomerase IV (consisting of *parC* and *parE*) (55), does not exhibit elevated mutation numbers in either the wild-type or the MMR$^-$ lines.

Because most of the MA lines acquired multiple mutations, direct links between specific mutations and norfloxacin resistance will need to be empirically tested with constructs developed by site-specific alterations, but the candidate mutations identified here at least provide a logical starting point for such work. In the next section, as a case study using site-directed mutagenesis, we confirm that one point mutation in the candidate resistance gene *marR* (the top gene in the wild-type candidate list) directly confers multidrug resistance.

Multidrug Resistance Caused by a Base Substitution Mutation. A G→A substitution in the wild-type line H43 (grown at 87.5 ng/mL) occurred at the third position of the start codon GTG of *marR* (genomic position 1,619,122; causing a fMet→valine amino acid change), possibly causing translation initiation failure of the gene, and this line has an evolved MIC for norfloxacin 4 times the ancestral level (Dataset S1, Table S2). *marR* is the repressor of the marABR operon, expression of which up-regulates the AcrAB efflux pump responsible for multidrug resistance in *E. coli* (56). Because there are two additional nonsynonymous mutations in other genes in this line (Dataset S1, Table S2), it is possible that this *marR* mutation is not the cause of the elevated resistance. However, introduction of the G→A point mutation into the wild-type progenitor by "scarless" site-directed mutagenesis (to produce the constructed line HL1) recapitulates the 4 times MIC elevation.

To evaluate whether this nonsynonymous mutation has general effects, we tested the MICs of HL1 to two other antibiotics: carbenicillin and chloramphenicol. This line has MICs of 32 μg/mL to both antibiotics, whereas parallel assay of the progenitor line reveals MICs of 16 μg/mL for chloramphenicol and 8 μg/mL for carbenicillin. The single G→A base substitution mutation in *marR* thus confers multiple-drug resistance to *E. coli*.

Coincidence of IS5-Mediated Duplications and *emrE* Efflux Pump Gene Expression Decrease. Using coverage analysis and quantitative PCR, we detected and validated large duplications in 21 lines, all in the 75 and 87.5 ng/mL treatments of wild-type lines (Fig. S4 and Dataset S1, Table S21). All duplications locate between genomic position 1 and 689,000, and most of these are 114 and 415 kb in size, with one exception of 689 kb in line G37. All of these duplications are flanked by IS5 elements, which are known to mediate chromosomal rearrangements by unequal homologous recombination (57) (Fig. S4), and it is notable that expression of the homologous-recombination pathway is significantly enriched upon norfloxacin treatment (Dataset S1, Table S12).

We find that all duplicated regions contain or flank an efflux pump gene *E. coli* multidrug resistance E (*emrE*) (Fig. S4, blue line), which belongs to the small multidrug resistance (SMR) family (58). Gene expression of wild-type *emrE* shows a negative correlation with norfloxacin concentration ($r = -0.81$, $P = 0.02$), and at concentrations ≥37.5 ng/mL is reduced to about half of the untreated expression level (Dataset S1, Table S8). It is plausible that the duplications of *emrE* may compensate for the expression decrease upon norfloxacin treatment, but knocking out or overexpressing *emrE* in *E. coli* in previous studies did not elicit norfloxacin resistance change (59, 60). Thus, the decrease in *emrE* expression may just be a coincidence, although there are numerous known cases of gene duplication/amplification related to the development of antibiotic resistance (61).

Discussion

This study has systematically evaluated the total pool of genomic mutations arising in 737 *E. coli* lines subjected to daily single-cell bottlenecks for 1–2 mo. After WGS, we detected thousands of mutational events, including point mutations, indels, prophage deletions, and large duplications, as well as their responses to sublethal concentrations of norfloxacin with or without the presence of DNA repair systems such as MMR and DNA oxidative-damage repair. Our findings demonstrate the power and resolution of MA techniques for ascertaining the consequences of exogenous factors for replication fidelity and damage repair, paving the way for future work on the mutagenic consequences of other antibiotics and other means of microbial intervention.

Numerous checks on the nature of mutations accumulated in this MA setting indicate that this experimental design cleanly separates the response of the mutation rate to antimicrobial dosage from the downstream issue of which specific mutations confer resistance. Because our mutation rate estimates experience negligible changes even after excluding the small subset of potential resistance-associated mutations, it appears clear that antibiotic exposure does not simply encourage the establishment of resistance by natural selection, but specifically increases the likelihood of the de novo emergence of the mutational fuel essential to such adaptation.

The large pool of mutations identified in our MA experiments may include a small subset of candidate resistance loci useful for future targets for drug discovery. For example, many mutations that we observed in known resistance-related genes such as *gyrA* and *gyrB* (Dataset S1, Table S20) are not in known quinolone resistance determining regions (QRDRs) (62), and they thus reveal a larger mutational space of the known target genes at low levels of norfloxacin treatments.

The fact that norfloxacin treatment globally elevates the mutation rates of all types of BPSs while also increasing the expression of low-fidelity polymerases suggests that antibiotic-associated mutation rate enhancement is at least part an indirect consequence of the cellular physiological response to stress (63). If this interpretation is correct, it implies that the application of all antimicrobials, regardless of their mode of action, may indirectly accelerate the rate of appearance of mutations conferring resistance simply by increasing the incidence of error-prone DNA replication. This raises the additional issue that stress-induced mutagenesis associated with the application of antibiotics may in the long run elevate the rate of appearance of adaptive mutations associated with other challenges confronted by pathogenic bacteria, e.g., host cell invasion and avoidance of host cell immune responses. The contribution of the SOS response to mutation elevation during norfloxacin treatment will be quantified by a running MA project using the wild-type and SOS-uninducible strains.

Comparisons of mutation rate responses to norfloxacin doses in wild-type lines with those of MMR^- and DNA oxidative-damage repair-deficient lines suggest that this drug also affects the efficiency of both postreplicative DNA mismatch and oxidative-damage repair. The influence of norfloxacin treatment on MMR efficiency corresponds well with a recent molecular genetic study on the negative effect of antibiotics on replication fidelity. Gutierrez et al. (64) showed that antibiotic treatment elevates the expression level of the global transcription regulator RpoS, which then induces expression of a small RNA (SdsR) that binds and represses the mRNA of MutS, a critical component of the MMR pathway, thereby causing mutation rate elevation. The mechanism by which norfloxacin affects DNA oxidative-damage repair needs further exploration.

Our results show that mutation-driven appearance of antibiotic resistance phenotypes increases more rapidly with norfloxacin concentration in mutator strains (the MMR^- lines) than in wild-type lines, with resistance mutations occasionally being acquired even in the absence of antibiotic treatment. Such observations correspond well with the widespread presence of MMR^- lines in clinical isolates of antibiotic-resistant strains (9). The maximum resistance level reached in this study (8 times ancestral MIC level or 1,000 ng/mL; Dataset S1, Tables S1 and S5) is the same in both the wild-type and MMR^- lines, which approximates the level of concentration following a typical clinical dosage: after orally taking 200 mg of norfloxacin, the peak concentration of this drug in serum is 750 ng/mL (37). Thus, the level of concern attached to the frequency of use and dosage levels of antibiotics is certainly justified (65, 66).

Although Kohanski et al. (23) found that mutation rates of norfloxacin-treated *E. coli* lines in liquid medium (estimated from fluctuation tests) correlate with an increase in ROS, we do not observe an elevation in the types of mutations expected to be elicited by ROS, e.g., G:C→T:A transversions in oxidation-sensitive mutant cells (Δ*mutY*) treated with norfloxacin. This discrepancy may be a result of the cells growing in different physiological conditions in the experiment of Kohanski et al. (23) and the current study, which may lead to different levels of oxygen exposure and/or degrees of ROS production, i.e., log-phase cells receiving high aeration in liquid medium shaken at high speed vs. heterogeneous cells in colonies on agar plates.

In summary, by revealing a large number of mutations in an unbiased way, the MA/WGS strategy provides a powerful approach to evaluating in a full genomic context the mutagenic consequences of antibiotics and other exogenous chemicals in ways not possible with reporter constructs, and in doing so provides a clear delineation between the separate issues of mutation and selection. Because the modes of action of antibiotics are diverse and microbes differ in their mechanisms of DNA repair, evaluation of the generality of our results will require the incorporation of such diversity in future research. Finally, the fact that antibiotics can act indirectly as bacterial mutagens raises the additional question of whether such exotic reagents may also have negative consequences for DNA stability in the cells of patients undergoing antibiotic treatment.

Materials and Methods

We ran single-colony daily transfers on three sets of *E. coli* K-12 MG1655 MA lines [wild-type, Δ*mutS*, Δ*mutY*; ancestor strains were kindly provided by Pat Foster's Laboratory (Indiana University, Bloomington, IN)] treated with gradients of norfloxacin for 1–2 mo (Table 1). We then constructed Illumina genome libraries and applied HiSeq 2500 WGS on each final evolved cell line. Mutations were then analyzed from MA lines after mapping reads to the reference genome (NC_000913.3). We also did RNA-seq on progenitor lines of wild-type and Δ*mutS* treated with or without norfloxacin, and measured resistance of the progenitor and the evolved lines by testing the MIC. Raw reads of genome sequencing and RNA-seq concerned in this study have been deposited in National Center for Biotechnology Information Sequence Read Archive with BioProject no. PRJNA301160 (study no. SRP066119). Details are in *SI Materials and Methods*.

ACKNOWLEDGMENTS. We thank Arnaud Gutierrez, Jacqueline Hernandez, Megan Behringer, Sen Xu, Graham Walker, Ellen Popodi, Brittany Niccum, Rebecca A. Zufall, Patricia L. Foster, Thomas G. Doak, Iain Konigsberg, Jie Huang, James Ford, Hayley Bedwell, Jiaqi Zheng, Tiffany H. C. Tsui, Xiaoqian Jiang, Way Sung, and Jean-Francois Gout for helpful discussions, technical support, and/or draft reading. We also thank the two reviewers for the insightful comments. This research was funded by Multidisciplinary University Research Initiative Award W911NF-09-1-0444 from the US Army Research Office and NIH Grant R01 GM036827.

1. Woodford N, Ellington MJ (2007) The emergence of antibiotic resistance by mutation. *Clin Microbiol Infect* 13(1):5–18.
2. Frana TS, et al. (2013) Isolation and characterization of methicillin-resistant *Staphylococcus aureus* from pork farms and visiting veterinary students. *PLoS One* 8(1):e53738.
3. Zurek L, Ghosh A (2014) Insects represent a link between food animal farms and the urban environment for antibiotic resistance traits. *Appl Environ Microbiol* 80(12):3562–3567.
4. Jobbins SE, Alexander KA (2015) From whence they came-antibiotic-resistant *Escherichia coli* in African wildlife. *J Wildl Dis* 51(4):811–820.
5. Lazarus B, Paterson DL, Mollinger JL, Rogers BA (2015) Do human extraintestinal *Escherichia coli* infections resistant to expanded-spectrum cephalosporins originate from food-producing animals? A systematic review. *Clin Infect Dis* 60(3):439–452.
6. Metz M, Shlaes DM (2014) Eight more ways to deal with antibiotic resistance. *Antimicrob Agents Chemother* 58(8):4253–4256.
7. Worth L, Jr, Clark S, Radman M, Modrich P (1994) Mismatch repair proteins MutS and MutL inhibit RecA-catalyzed strand transfer between diverged DNAs. *Proc Natl Acad Sci USA* 91(8):3238–3241.
8. de Visser JA (2002) The fate of microbial mutators. *Microbiology* 148(Pt 5):1247–1252.
9. Oliver A, Cantón R, Campo P, Baquero F, Blázquez J (2000) High frequency of hypermutable *Pseudomonas aeruginosa* in cystic fibrosis lung infection. *Science* 288(5469):1251–1254.
10. Gerrish PJ, Colato A, Perelson AS, Sniegowski PD (2007) Complete genetic linkage can subvert natural selection. *Proc Natl Acad Sci USA* 104(15):6266–6271.
11. Giraud A, Matic I, Radman M, Fons M, Taddei F (2002) Mutator bacteria as a risk factor in treatment of infectious diseases. *Antimicrob Agents Chemother* 46(3):863–865.
12. Jørgensen KM, et al. (2013) Sublethal ciprofloxacin treatment leads to rapid development of high-level ciprofloxacin resistance during long-term experimental evolution of *Pseudomonas aeruginosa*. *Antimicrob Agents Chemother* 57(9):4215–4221.
13. Blázquez J, Couce A, Rodríguez-Beltrán J, Rodríguez-Rojas A (2012) Antimicrobials as promoters of genetic variation. *Curr Opin Microbiol* 15(5):561–569.
14. Shen LL, et al. (1989) Mechanism of inhibition of DNA gyrase by quinolone antibacterials: A cooperative drug–DNA binding model. *Biochemistry* 28(9):3886–3894.
15. Hooper DC, et al. (1986) Genetic and biochemical characterization of norfloxacin resistance in *Escherichia coli*. *Antimicrob Agents Chemother* 29(4):639–644.

16. Crumplin GC, Kenwright M, Hirst T (1984) Investigations into the mechanism of action of the antibacterial agent norfloxacin. *J Antimicrob Chemother* 13(Suppl B):9–23.
17. Kunkel TA (2009) Evolving views of DNA replication (in)fidelity. *Cold Spring Harb Symp Quant Biol* 74:91–101.
18. Phillips I, Culebras E, Moreno F, Baquero F (1987) Induction of the SOS response by new 4-quinolones. *J Antimicrob Chemother* 20(5):631–638.
19. Radman M (1975) SOS repair hypothesis: Phenomenology of an inducible DNA repair which is accompanied by mutagenesis. *Basic Life Sci* 5A:355–367.
20. Drlica K, Malik M, Kerns RJ, Zhao X (2008) Quinolone-mediated bacterial death. *Antimicrob Agents Chemother* 52(2):385–392.
21. Galhardo RS, et al. (2009) DinB upregulation is the sole role of the SOS response in stress-induced mutagenesis in *Escherichia coli*. *Genetics* 182(1):55–68.
22. Napolitano R, Janel-Bintz R, Wagner J, Fuchs RP (2000) All three SOS-inducible DNA polymerases (Pol II, Pol IV and Pol V) are involved in induced mutagenesis. *EMBO J* 19(22):6259–6265.
23. Kohanski MA, DePristo MA, Collins JJ (2010) Sublethal antibiotic treatment leads to multidrug resistance via radical-induced mutagenesis. *Mol Cell* 37(3):311–320.
24. Dwyer DJ, Collins JJ, Walker GC (2015) Unraveling the physiological complexities of antibiotic lethality. *Annu Rev Pharmacol Toxicol* 55:313–332.
25. Dwyer DJ, et al. (2014) Antibiotics induce redox-related physiological alterations as part of their lethality. *Proc Natl Acad Sci USA* 111(20):E2100–E2109.
26. López E, Elez M, Matic I, Blázquez J (2007) Antibiotic-mediated recombination: Ciprofloxacin stimulates SOS-independent recombination of divergent sequences in *Escherichia coli*. *Mol Microbiol* 64(1):83–93.
27. Lee H, Popodi E, Tang H, Foster PL (2012) Rate and molecular spectrum of spontaneous mutations in the bacterium *Escherichia coli* as determined by whole-genome sequencing. *Proc Natl Acad Sci USA* 109(41):E2774–E2783.
28. Sung W, et al. (2015) Asymmetric context-dependent mutation patterns revealed through mutation-accumulation experiments. *Mol Biol Evol* 32(7):1672–1683.
29. Drake JW (1991) A constant rate of spontaneous mutation in DNA-based microbes. *Proc Natl Acad Sci USA* 88(16):7160–7164.
30. Stewart FM (1994) Fluctuation tests: How reliable are the estimates of mutation rates? *Genetics* 137(4):1139–1146.
31. Kibota TT, Lynch M (1996) Estimate of the genomic mutation rate deleterious to overall fitness in *E. coli*. *Nature* 381(6584):694–696.
32. Lynch M, et al. (2008) A genome-wide view of the spectrum of spontaneous mutations in yeast. *Proc Natl Acad Sci USA* 105(27):9272–9277.
33. Farlow A, et al. (2015) The spontaneous mutation rate in the fission yeast *Schizosaccharomyces pombe*. *Genetics* 201(2):737–744.
34. Morgan AD, Ness RW, Keightley PD, Colegrave N (2014) Spontaneous mutation accumulation in multiple strains of the green alga, *Chlamydomonas reinhardtii*. *Evolution* 68(9):2589–2602.
35. Sung W, Ackerman MS, Miller SF, Doak TG, Lynch M (2012) Drift-barrier hypothesis and mutation-rate evolution. *Proc Natl Acad Sci USA* 109(45):18488–18492.
36. Foti JJ, Devadoss B, Winkler JA, Collins JJ, Walker GC (2012) Oxidation of the guanine nucleotide pool underlies cell death by bactericidal antibiotics. *Science* 336(6079):315–319.
37. Swanson BN, Boppana VK, Vlasses PH, Rotmensch HH, Ferguson RK (1983) Norfloxacin disposition after sequentially increasing oral doses. *Antimicrob Agents Chemother* 23(2):284–288.
38. Halligan DL, Keightley PD (2009) Spontaneous mutation accumulation studies in evolutionary genetics. *Annu Rev Ecol Evol Syst* 40:151–172.
39. Long H, et al. (2015) Background mutational features of the radiation-resistant bacterium *Deinococcus radiodurans*. *Mol Biol Evol* 32(9):2383–2392.
40. Wijker CA, Lafleur MV (1998) Influence of the UV-activated SOS response on the gamma-radiation-induced mutation spectrum in the lacI gene. *Mutat Res* 408(3):195–201.
41. Foster PL, Eisenstadt E (1985) Induction of transversion mutations in *Escherichia coli* by *N*-methyl-*N*′-nitro-*N*-nitrosoguanidine is SOS dependent. *J Bacteriol* 163(1):213–220.
42. Modrich P, Lahue R (1996) Mismatch repair in replication fidelity, genetic recombination, and cancer biology. *Annu Rev Biochem* 65:101–133.
43. Fijalkowska IJ, Dunn RL, Schaaper RM (1997) Genetic requirements and mutational specificity of the *Escherichia coli* SOS mutator activity. *J Bacteriol* 179(23):7435–7445.
44. Courcelle J, Khodursky A, Peter B, Brown PO, Hanawalt PC (2001) Comparative gene expression profiles following UV exposure in wild-type and SOS-deficient *Escherichia coli*. *Genetics* 158(1):41–64.
45. Greener A, Hill CW (1980) Identification of a novel genetic element in *Escherichia coli* K-12. *J Bacteriol* 144(1):312–321.
46. Reif HJ, Saedler H (1975) IS1 is involved in deletion formation in the *gal* region of *E. coli* K12. *Mol Gen Genet* 137(1):17–28.
47. Curti E, McDonald JP, Mead S, Woodgate R (2009) DNA polymerase switching: Effects on spontaneous mutagenesis in *Escherichia coli*. *Mol Microbiol* 71(2):315–331.
48. Schaaper RM, Dunn RL (1987) Spectra of spontaneous mutations in *Escherichia coli* strains defective in mismatch correction: The nature of in vivo DNA replication errors. *Proc Natl Acad Sci USA* 84(17):6220–6224.
49. Gogos A, Cillo J, Clarke ND, Lu AL (1996) Specific recognition of A/G and A/7,8-dihydro-8-oxoguanine (8-oxoG) mismatches by *Escherichia coli* MutY: Removal of the C-terminal domain preferentially affects A/8-oxoG recognition. *Biochemistry* 35(51):16665–16671.
50. Michaels ML, Cruz C, Grollman AP, Miller JH (1992) Evidence that MutY and MutM combine to prevent mutations by an oxidatively damaged form of guanine in DNA. *Proc Natl Acad Sci USA* 89(15):7022–7025.
51. Grollman AP, Moriya M (1993) Mutagenesis by 8-oxoguanine: An enemy within. *Trends Genet* 9(7):246–249.
52. Foster PL, Lee H, Popodi E, Townes JP, Tang H (2015) Determinants of spontaneous mutation in the bacterium *Escherichia coli* as revealed by whole-genome sequencing. *Proc Natl Acad Sci USA* 112(44):E5990–E5999.
53. Yoon SH, et al. (2003) MutY is down-regulated by oxidative stress in *E. coli*. *Free Radic Res* 37(8):873–879.
54. Drlica K, Zhao X (1997) DNA gyrase, topoisomerase IV, and the 4-quinolones. *Microbiol Mol Biol Rev* 61(3):377–392.
55. Hooper DC (1999) Mechanisms of fluoroquinolone resistance. *Drug Resist Updat* 2(1):38–55.
56. Okusu H, Ma D, Nikaido H (1996) AcrAB efflux pump plays a major role in the antibiotic resistance phenotype of *Escherichia coli* multiple-antibiotic-resistance (Mar) mutants. *J Bacteriol* 178(1):306–308.
57. Umeda M, Ohtsubo E (1990) Mapping of insertion element IS5 in the *Escherichia coli* K-12 chromosome. Chromosomal rearrangements mediated by IS5. *J Mol Biol* 213(2):229–237.
58. Yerushalmi H, Lebendiker M, Schuldiner S (1995) EmrE, an *Escherichia coli* 12-kDa multidrug transporter, exchanges toxic cations and H^+ and is soluble in organic solvents. *J Biol Chem* 270(12):6856–6863.
59. Sulavik MC, et al. (2001) Antibiotic susceptibility profiles of *Escherichia coli* strains lacking multidrug efflux pump genes. *Antimicrob Agents Chemother* 45(4):1126–1136.
60. Nishino K, Yamaguchi A (2001) Analysis of a complete library of putative drug transporter genes in *Escherichia coli*. *J Bacteriol* 183(20):5803–5812.
61. Sandegren L, Andersson DI (2009) Bacterial gene amplification: Implications for the evolution of antibiotic resistance. *Nat Rev Microbiol* 7(8):578–588.
62. Yoshida H, Bogaki M, Nakamura M, Nakamura S (1990) Quinolone resistance-determining region in the DNA gyrase *gyrA* gene of *Escherichia coli*. *Antimicrob Agents Chemother* 34(6):1271–1272.
63. MacLean RC, Torres-Barceló C, Moxon R (2013) Evaluating evolutionary models of stress-induced mutagenesis in bacteria. *Nat Rev Genet* 14(3):221–227.
64. Gutierrez A, et al. (2013) β-Lactam antibiotics promote bacterial mutagenesis via an RpoS-mediated reduction in replication fidelity. *Nat Commun* 4:1610.
65. Levy S (2002) *The Antibiotic Paradox: How Misuse of Antibiotics Destroys Their Curative Powers* (Perseus, Cambridge, MA).
66. Joshi N, Milfred D (1995) The use and misuse of new antibiotics. A perspective. *Arch Intern Med* 155(6):569–577.
67. Blank K, Hensel M, Gerlach RG (2011) Rapid and highly efficient method for scarless mutagenesis within the *Salmonella enterica* chromosome. *PLoS One* 6(1):e15763.
68. Andrews JM (2001) Determination of minimum inhibitory concentrations. *J Antimicrob Chemother* 48(Suppl 1):5–16.
69. Wahl LM, Gerrish PJ (2001) The probability that beneficial mutations are lost in populations with periodic bottlenecks. *Evolution* 55(12):2606–2610.
70. Bolger AM, Lohse M, Usadel B (2014) Trimmomatic: A flexible trimmer for Illumina sequence data. *Bioinformatics* 30(15):2114–2120.
71. Li H, Durbin R (2009) Fast and accurate short read alignment with Burrows-Wheeler transform. *Bioinformatics* 25(14):1754–1760.
72. DePristo MA, et al. (2011) A framework for variation discovery and genotyping using next-generation DNA sequencing data. *Nat Genet* 43(5):491–498.
73. McKenna A, et al. (2010) The Genome Analysis Toolkit: A MapReduce framework for analyzing next-generation DNA sequencing data. *Genome Res* 20(9):1297–1303.
74. Chen K, et al. (2009) BreakDancer: An algorithm for high-resolution mapping of genomic structural variation. *Nat Methods* 6(9):677–681.
75. Ye K, Schulz MH, Long Q, Apweiler R, Ning Z (2009) Pindel: A pattern growth approach to detect break points of large deletions and medium sized insertions from paired-end short reads. *Bioinformatics* 25(21):2865–2871.
76. Lee H, Popodi E, Foster PL, Tang H (2014) Detection of structural variants involving repetitive regions in the reference genome. *J Comput Biol* 21(3):219–233.
77. Livak KJ, Schmittgen TD (2001) Analysis of relative gene expression data using real-time quantitative PCR and the 2(−Delta Delta C(T)) method. *Methods* 25(4):402–408.
78. Yuan JS, Reed A, Chen F, Stewart CN, Jr (2006) Statistical analysis of real-time PCR data. *BMC Bioinformatics* 7:85.
79. Trapnell C, Pachter L, Salzberg SL (2009) TopHat: Discovering splice junctions with RNA-Seq. *Bioinformatics* 25(9):1105–1111.
80. Trapnell C, et al. (2010) Transcript assembly and quantification by RNA-Seq reveals unannotated transcripts and isoform switching during cell differentiation. *Nat Biotechnol* 28(5):511–515.
81. Huang W, Sherman BT, Lempicki RA (2009) Systematic and integrative analysis of large gene lists using DAVID bioinformatics resources. *Nat Protoc* 4(1):44–57.
82. R Development Core Team (2014) *R: A Language and Environment for Statistical Computing* (R Foundation for Statistical Computing, Vienna).
83. Wickham H (2009) *ggplot2: Elegant Graphics for Data Analysis* (Springer, New York).

Supporting Information

Long et al. 10.1073/pnas.1601208113

SI Materials and Methods

Strains, Media, and Antibiotics. All wild-type (laboratory designation name, PFM2), *ΔmutY* (PFM6), *ΔmutS* (PFM342), and *marR*:M1V (HL1, with *marR* G→A base substitution at genomic site 1,619,122) strains were in the K-12 MG1655 background. Mutant strains were constructed using "scarless" site-directed mutagenesis and verified by Sanger sequencing. This protocol combined the λ Red recombinase system with selection using the I-SceI endonuclease after transformation without introducing a selective marker (67).

Stock solutions of norfloxacin (catalog no. N9890-5G; Sigma-Aldrich), chloramphenicol (C0378-25G; Sigma-Aldrich), and carbenicillin (C3416-1G; Sigma-Aldrich) were made according to the manufacturers' instructions. LB agar plates used for passaging were prepared by adding 1 mg/mL stock norfloxacin in 10% (vol/vol) acetic acid. All of the vehicle controls and treatments were also supplemented with 10% acetic acid as necessary to control pH.

MIC Tests. We used a protocol modified from Andrews (68): cells were cultured on a tissue culture rotator for about 17 h to $OD_{650} \sim 1$. Culture was then serially diluted and about 1,500 cells were plated onto LB plates with norfloxacin: 0, 62.5, 125, 250, 500, 1,000, and 2,000 ng/mL. The concentration gradients used for testing chloramphenicol and carbenicillin resistance were as follows: 0, 1, 2, 4, 8, 16, 32, and 64 μg/mL. Colony presence was then visually identified after 24 h, and the average MIC of the three replicates for each tested line was then calculated.

Efficiency of Plating upon Norfloxacin Treatments. Cells were cultured overnight (~17 h) and then serially diluted. About 1,500 cells were then plated onto LB plates containing 0, 12.5, 25, 37.5, 50, 62.5, 75, 87.5, 100, and 125 ng/mL norfloxacin, with six replicates at each concentration. Colony-forming units were then counted after 24 h at 37 °C. EOP was then calculated by dividing the colony-forming units with that from the blank control.

Experimental Design and Transfers. Eight groups of wild-type cell lines treated with a 12.5 ng/mL progression of norfloxacin concentrations (A: 0 ng/mL; B: 12.5; C: 25; D or XD: 37.5; E: 50; F: 62.5; G: 75; H: 87.5) were all initiated from a single wild-type colony. Each group included 48 replicate cell lines, as a large number of cell lines were needed to accumulate mutations even under antibiotics treatments. Lines were transferred daily (24 h) and incubated at 37 °C and transferred by streaking single colonies onto fresh LB agar plates (Table 1).

Another eight groups of *ΔmutS* lines treated with the above norfloxacin concentrations (designated as SA, SB, SC, SD, SE, SF, SG, and SH) were initiated from a single *ΔmutS* colony. The *ΔmutS* cell lines were transferred similarly for 27–28 d, with the exception of group SD, which were transferred for 61 d due to mislabeling (detected after whole-genome sequencing). Each group included 12 cell lines (Table 1).

Effective population size (N_e; Table 1) of each treatment was calculated by taking the harmonic mean of successive doublings from population size of 1 until the final population size is reached (69).

All *ΔmutY* cell lines also shared a single-cell progenitor and two sets of experiments were done at different time points. For the first set, 19 lines of the four norfloxacin treatments were single-colony transferred 73 times: 0 (designated as YA), 3.125 (YB), 12.5 (YC), and 50 (YF) ng/mL. In addition, 20 lines of the positive control were treated with 20 mM H_2O_2 and transferred for 48 d. Because H_2O_2 decomposes in melted agar, the 20 mM H_2O_2 solution was first spread onto plain LB agar before streaking. For the second set, 48 lines of the following four norfloxacin treatments were transferred 30 times: 25 (YD), 37.5 (YE), 75 (YG), and 87.5 ng/mL (YH).

We estimated the number of cell divisions about every 3 wk. For each group, single colonies from about five randomly selected cell lines were cut from agar plates, serially diluted in 1× PBS, plated, and then colony-forming units N was counted. The cell division number between transfers was then calculated by $\log_2 N$, assuming exponential growth. The overall mean number of cell divisions between transfers across the whole experiment multiplied by the number of transfers was then used as the cell division estimate passed for each line.

DNA Extraction, Library Construction, and Genome Sequencing. The genomic DNA was extracted with the Wizard Genomic DNA Purification Kit (Promega). Nextera DNA Library Preparation Kit (Illumina) was used to construct libraries for Illumina HiSeq 2500 sequencing with an insert size of 300 bp. The 150-bp paired-end sequencing of evolved lines was done by the Hubbard Center for Genome Studies, University of New Hampshire (Durham, NH), with median depths of coverage of 77 times (wild type), 68 times (*ΔmutS*), and 92 times (*ΔmutY*), after excluding cross-contaminated or <20 times coverage lines.

Mutation Analyses. After trimming library adaptors of paired-end reads with Trimmomatic 0.32 (70), we applied a modified consensus approach to identify base pair substitutions and indels (28), using BWA, version 0.7.10 (71), to map unique high-quality reads to the reference genome (National Center for Biotechnology Information accession no. NC_000913.3). We also applied duplicate reads removal and reads realignment around indels using GATK (72, 73). False positives due to mismapping or possible recombination were excluded from the study as shown in Dataset S1, Table S22. Mutation rate μ is calculated by the following: $\mu = m/\sum_1^n N \times T$, where m is the total number of mutations across all MA lines, n is the total number of lines, N is the analyzed sites in one line, and T is the number of cell divisions passed in the MA process of the line. Standard error of the mean mutation rate is calculated with the following: $\mathrm{SEM} = \mathrm{SD}/\sqrt{n}$, where SD is the standard deviation of the line-specific mutation rates.

BreakDancer 1.1.2 (74) and Pindel 0.2.4w (75) were also applied to detect both large and small indels' breakpoints and realign reads to reduce false positives. In addition to BreakDancer/Pindel, we detected large deletions (e.g., e14 prophage excision; IS1-mediated CP4-6 deletions) and duplications using the depth of coverage information and constructed a coverage matrix for each group of evolved lines. The distribution of target regions' coverage was also visualized by a 1-kb sliding window with 500-bp step. Candidate duplications were also validated by quantitative PCR (see details below).

We analyzed IS element insertions through transposition in the wild-type and *ΔmutS* evolved lines that occurred during transfers using GRASPER (https://github.com/COL-IU/GRASPER), which constructed an A_l-*Bruijn* graph (l = 90, error rate of 5%) based on the algorithms described in Lee et al. (76). For each cell line, paired-end reads were mapped and SAM-formatted using BWA and loaded onto the graph to first select discordant read pairs inferring novel insertions of IS elements during evolution. We define discordant clusters as any clusters with ≥10 discordant read-pairs. Based on these clusters, we analyzed deletions mediated by homologous recombination of IS elements and duplicative

insertions of IS elements. Using this method, we also analyzed other non-IS structural variants like e14 prophage excisions and CP4-6 deletions to supplement the above BreakDancer/Pindel and coverage analyses.

Quantitative PCR. To validate duplications detected by the coverage analysis, we designed primers targeting the internal reference region (1,999,678–1,999,869): 678F-5′-CAGCAGGTCCTCATTTCCTTTA-3′, 678R-5′-GTGCGTACCTATGATGATGACC-3′, which is confirmed to be nonrepetitive by a lack of highly similar hits from blasting the whole genome. The target region (578,500–579,000) was shared by all detected duplicated regions of the tested 25 evolved lines (Dataset S1, Table S21), and primers were as follows: 8500F-5′-CTGCATCGACAGTTTTCTTCTG-3′, 8500R-5′-ACTTCAAAAAGCATCGGGAATA-3′. The wild-type progenitor line was used as the control line and three replicates were prepared for all of the control and evolved lines. Quantitative PCR reactions used PerfeCTa SYBR Green FastMix (Quanta Biosciences) PCR kit on a Stratagene Mx3000P. The $2^{-\Delta\Delta CT}$ method and *t* tests were used to analyze the copy number data (77, 78).

RNA-seq. We streaked both wild-type and Δ*mutS* progenitor cells onto LB plates and cultured overnight at 37 °C. Single colonies were then streaked onto LB plates with the following norfloxacin doses, with three replicates each: 0, 12.5, 25, 37.5, 50, 62.5, 75, and 87.5 ng/mL. After 24 h incubation at 37 °C, cells on each plate were then scraped off and transferred to Eppendorf tubes. Total RNA was then extracted using the FastRNA Blue Kit (MP Biomedicals) and cleaned with the RNeasy Mini kit (Qiagen). RNA-seq libraries were then constructed using the ScriptSeq Complete Kit (Bacteria) (Illumina) and TruSeq RNA Library Preparation Kits (Illumina) by Center for Genomics and Bioinformatics (CGB), Indiana University. The 150-bp paired-end reads of the wild-type lines were obtained from a HiSeq 2500 at the Hubbard Center for Genome Studies, University of New Hampshire; 75-bp single-end reads of the Δ*mutS* lines were from a NextSeq at CGB, Indiana University. Reads were then mapped with Tophat2 (79), and gene expression levels in each group were analyzed using Cufflinks 2.2.1 (80). Each wild-type replicate had on average 1.60 million (SD = 0.83 million) reads, and each Δ*mutS* replicate had 6.61 million (SD = 2.31 million) reads successfully mapped to the transcriptome. Gene enrichment analyses were then done on list of genes with significantly different expression levels from the negative control (0 ng/mL) in each treatment, using Database for Annotation, Visualization, and Integrated Discovery (DAVID), version 6.7 (81).

Statistics and Plotting. All statistics were done in R 3.1.3 (82) and Mathematica 10.1, and plotting was done using R package ggplot2 (83).

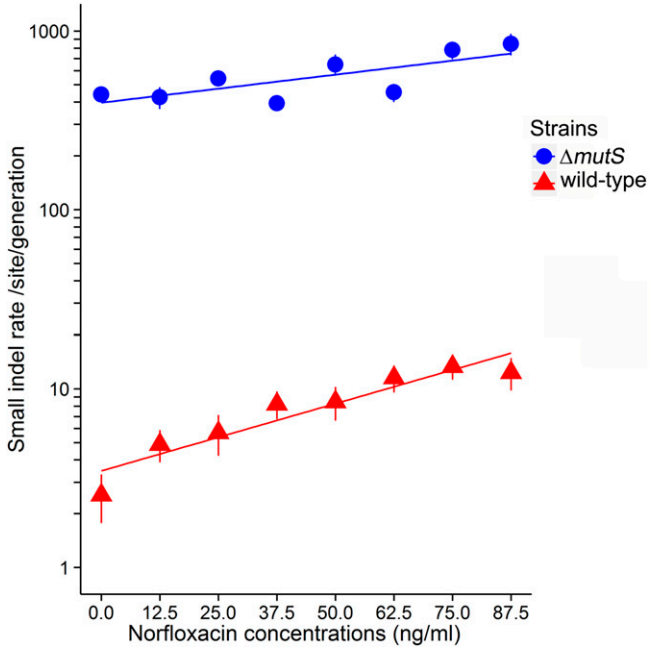

Fig. S1. Small indel rate at different norfloxacin concentrations in both wild-type and Δ*mutS* evolved lines.

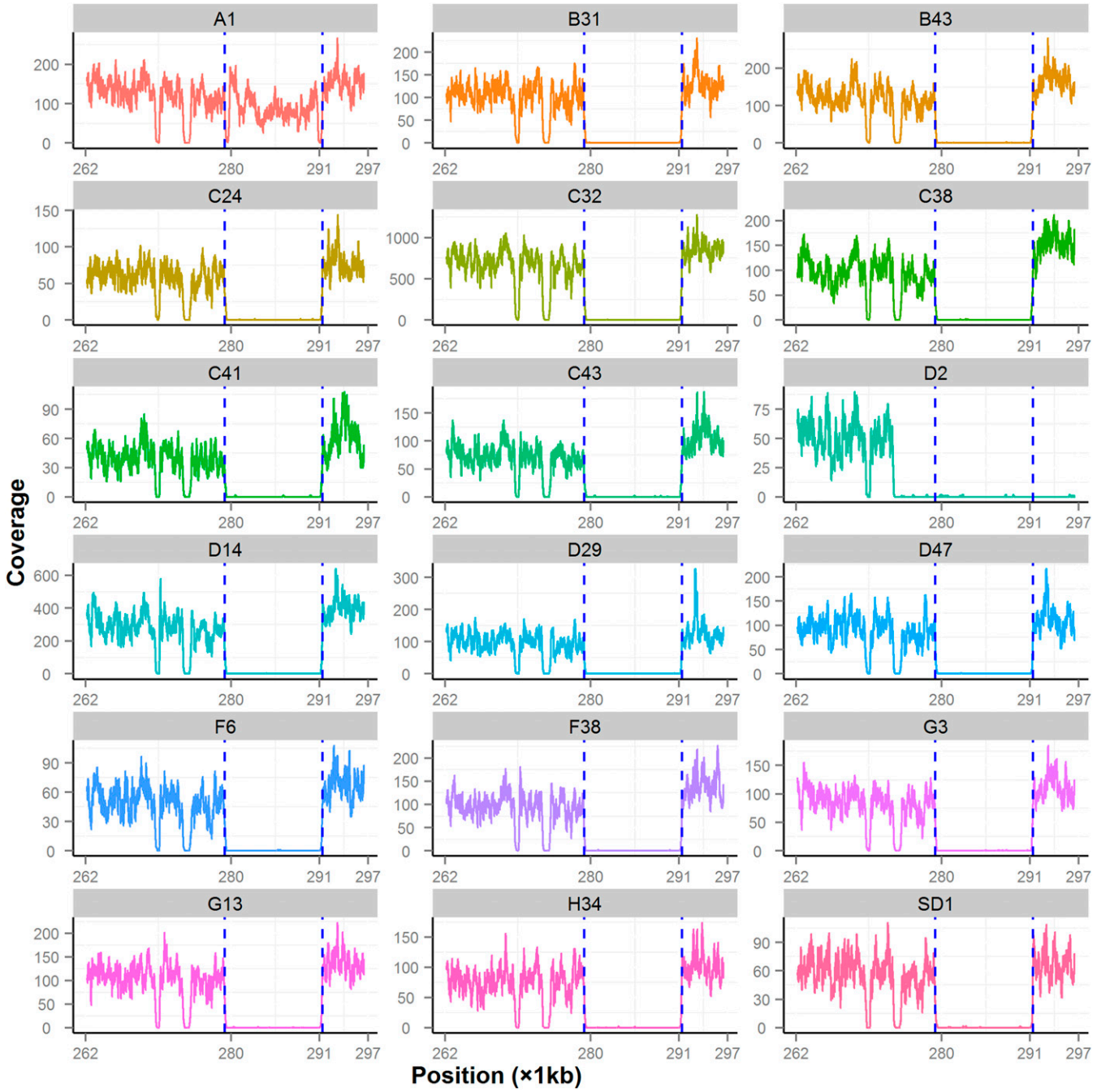

Fig. S2. All detected large deletions mediated by IS1 recombination in CP4-6 prophages. Blue dashed lines show IS1 elements positions; line A1 is a control line without CP4-6 deletion.

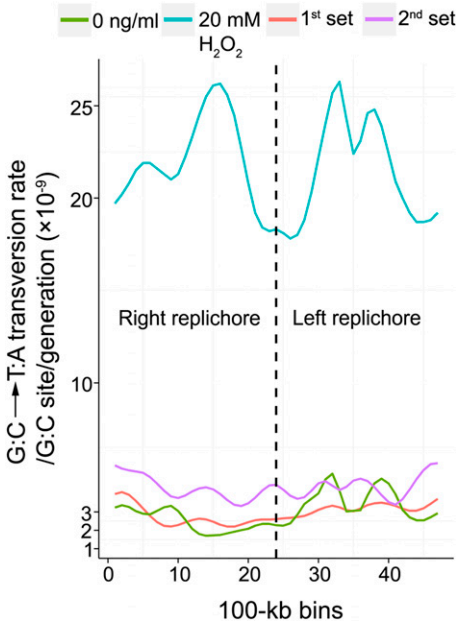

Fig. S3. Distribution of G:C→T:A transversion rate across the genome (in 100-kb bins; bin 1 starts from the origin of replication) after fourth-order Daubechies wavelet transformation. The first set denotes pooled G:C→T:A transversions of the first set of experiments (*mutY* lines treated with 0, 3.125, 12.5, 50 ng/mL norfloxacin), and the second set denotes the second set of experiments (*mutY* lines treated with 25, 37.5, 75, 87.5 ng/mL norfloxacin).

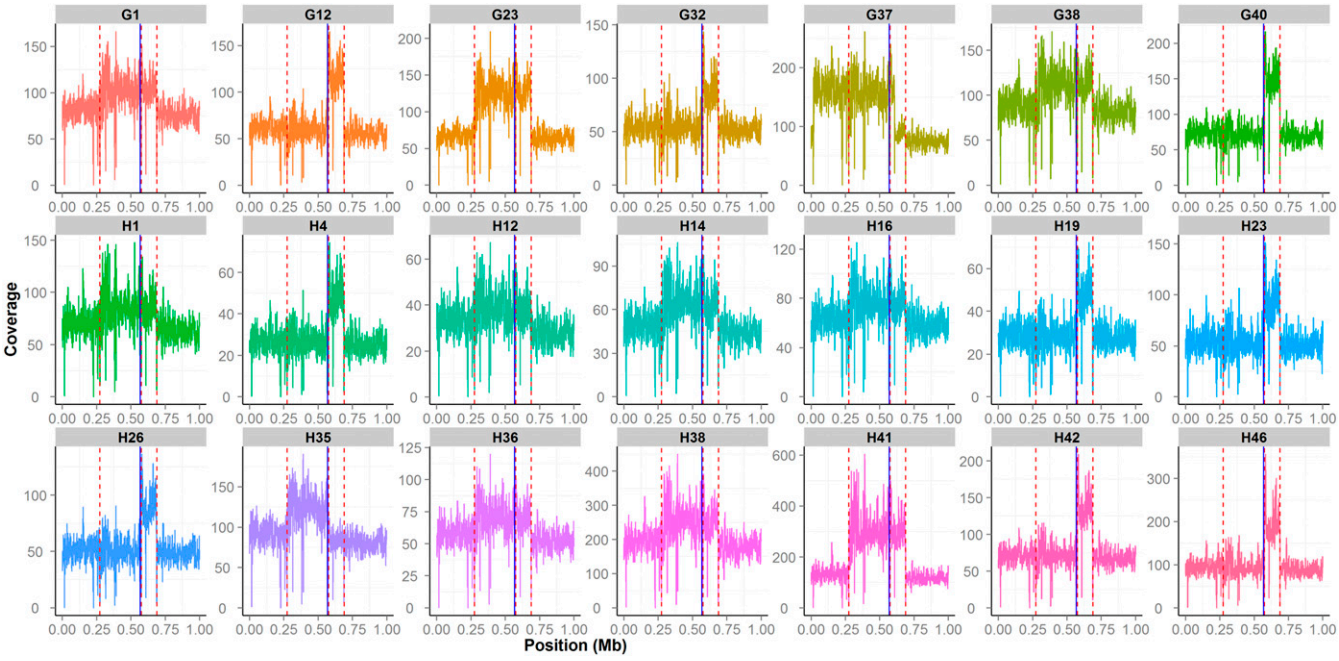

Fig. S4. Validated duplications mediated by IS5. Red dashed lines show IS5 elements' positions; blue vertical lines show *emrE* position.

Other Supporting Information Files

Dataset S1 (XLSX)